



HIGH RESOLUTION XMM-NEWTON SPECTROSCOPY OF A COOLING FLOW CLUSTER A3112



G. Esra Bulbul¹,

Randall Smith¹, Adam Foster¹, Jean Cottam², Michael Loewenstein², Richard Mushotzky², Richard Shafer²

1. Introduction

XMM-Newton and Chandra observations have revealed that some process inhibits gas cooling and falling onto central cD galaxies. Understanding what happened to the cool gas in cooling flow clusters was one of the prime problems in extragalactic astrophysics until analysis of the XMM-Newton RGS spectra showed that they do not, in fact, cool beyond a temperature about one-third of the virial temperature. We examine the high signal-to-noise XMM-Newton EPIC and RGS observations to determine the physical characteristics of gas in the cool core and outskirts of the nearby rich cluster A3112.

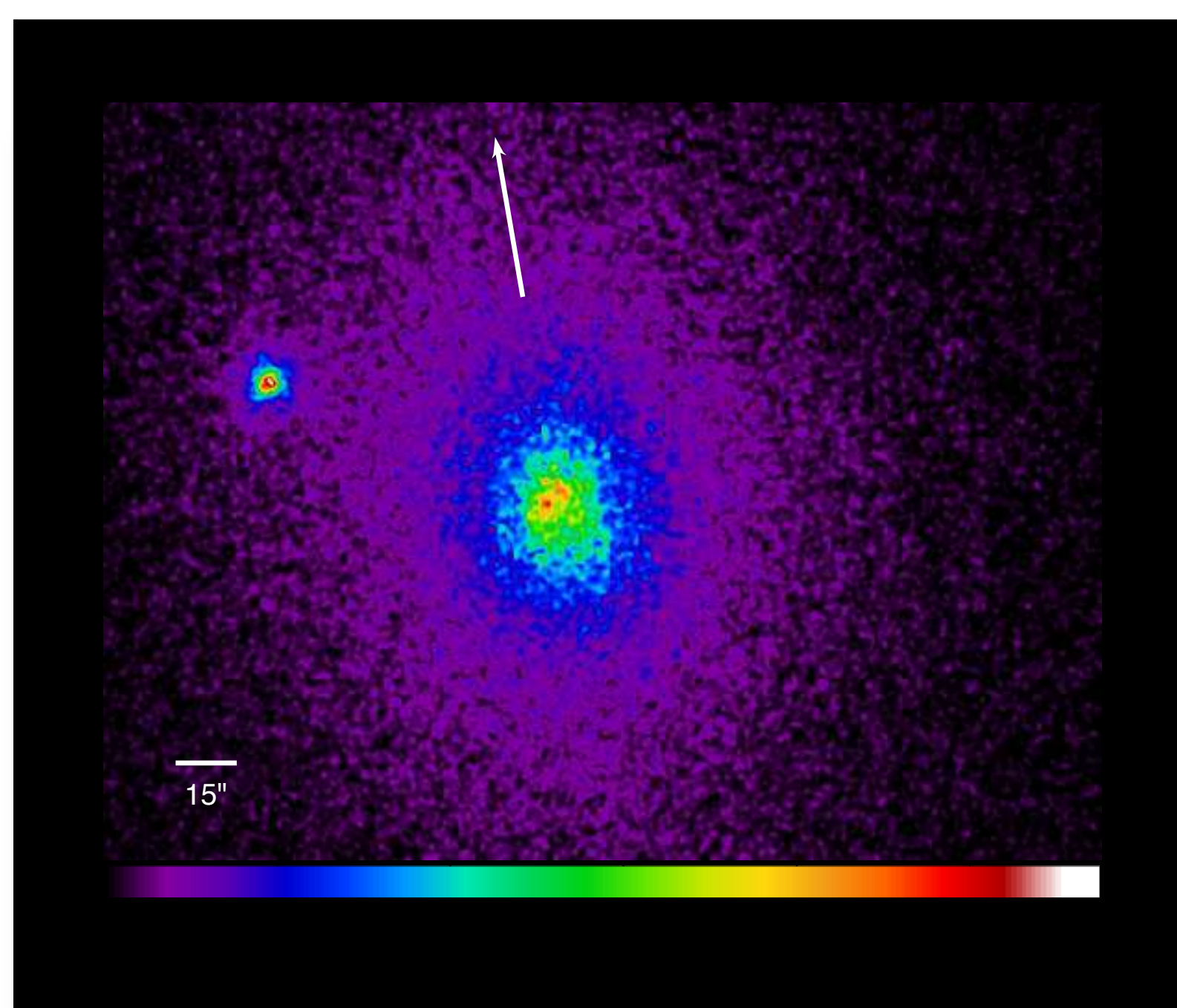


Figure 1. XMM-Newton Image of Abell 3112.

1. XMM-Newton EPIC Observations

Abell 3112 was observed with XMM-Newton in July 2009 for 119 ksec and August 2009 for 80 ksec. The EPIC data processing and background modeling was carried out with the XMM-Newton Extended Source Analysis Software (XMM-ESAS) and methods (Kuntz & Snowden 2008; Snowden et al. 2008). Proper treatment of the background, along with cross talk effects, are the keys to XMM-Newton observations of extended sources. The proper background components used in our XMM-Newton MOS and PN data analysis are:

1. Instrumental Background (Al K α , Si K α Lines)
2. Cosmic X-ray Background
3. Potential Solar Wind Charge Exchange Emission
4. Cross-Talk Correction

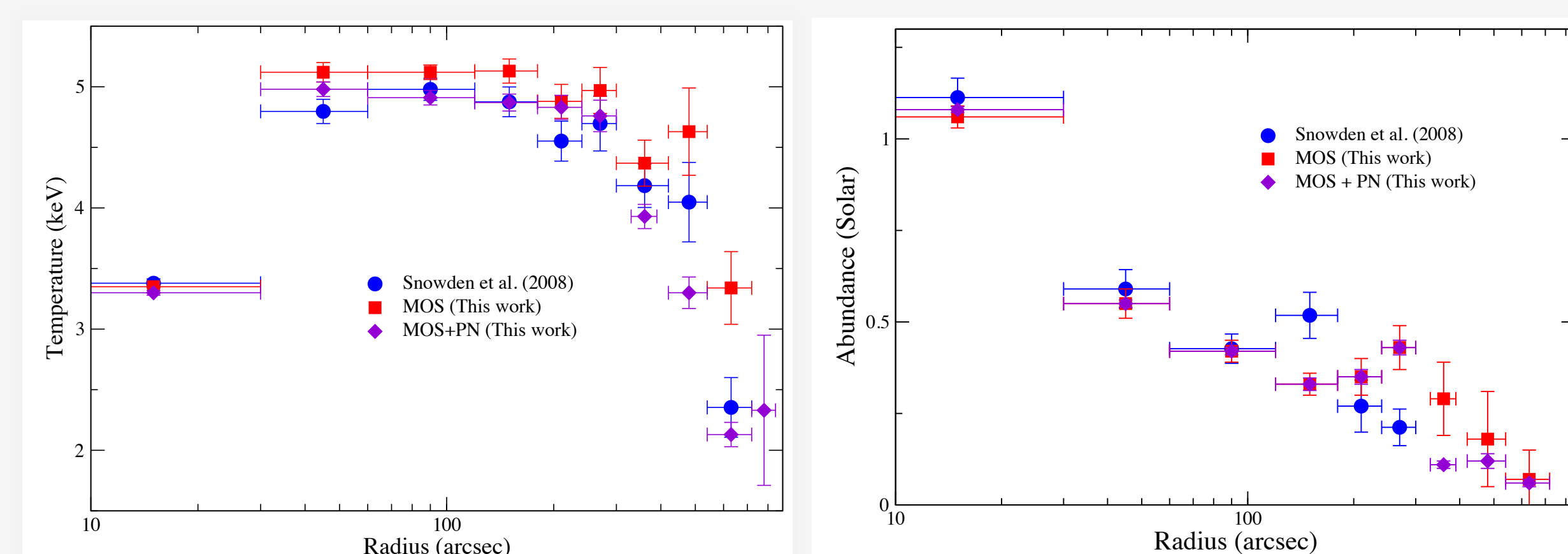


Figure 2. The best fit abundance and temperature measurements of A3112 obtained from MOS is shown in red, MOS and PN are shown in purple. The blue data points are the measurements reported in Snowden et al. (2008).

Summary

- ◉ We find that MOS temperature measurements are systematically higher than MOS+PN combined temperatures. The systematic discrepancy in the wide band temperatures up to 6% was also observed by Nevalainen et al. (2010). The abundance measurements obtained from the MOS observations are in good agreement with those obtained from the MOS+PN observations and the Snowden et al. (2008) results (see Figure 2).
- ◉ The centrally peaked trend of Fe and Si qualitatively is consistent with the idea that the contribution from SNe Ia towards the cluster center, while the distribution of SNe II remains more or less uniform (see Figure 3) (Kaastra et al. 2001; Tamura et al. 2004).
- ◉ At r_{500} , the total mass $M=(3.00\pm 0.59)\times 10^{14} M_{\text{sun}}$, is in agreement with the results of Nulsen et al. (2010), and the total mass derived from $M_{\text{tot}}-T$ scaling relations (Arnaud et al. 2005). The gas mass fraction is, $f_{\text{gas}}=0.149\pm 0.036$ at r_{500} is consistent with the 7 year WMAP cosmic baryon fraction, $\Omega_b/\Omega_M=0.167$ (Komatsu et al. 2011).
- ◉ The 90 per cent upper limit to line-of-sight, non-thermal, velocity broadening is 220 km s^{-1} , measured from the emission lines originating within 38 arcsecond radius (see Figure 5). The ratio of turbulent to thermal energy density in the core is therefore less than 13.7 per cent. This is among the lowest limits in Sanders et al. (2011) sample.
- ◉ The 90% upper limits to the Fe XVII and FeVIII line fluxes in the RGS spectra proves the absence of $< 1 \text{ keV}$ gas in the center (see Figure 6). This implies that the soft excess emission previously detected from this cluster does not have a thermal origin.

- ◉ The MOS temperature measurements are systematically higher than MOS+PN combined temperatures. The systematic discrepancy in the wide band temperatures up to 6% was also observed by Nevalainen et al. (2010). The abundance measurements obtained from the MOS observations are in good agreement with those obtained from the MOS+PN observations and the Snowden et al. (2008) results.

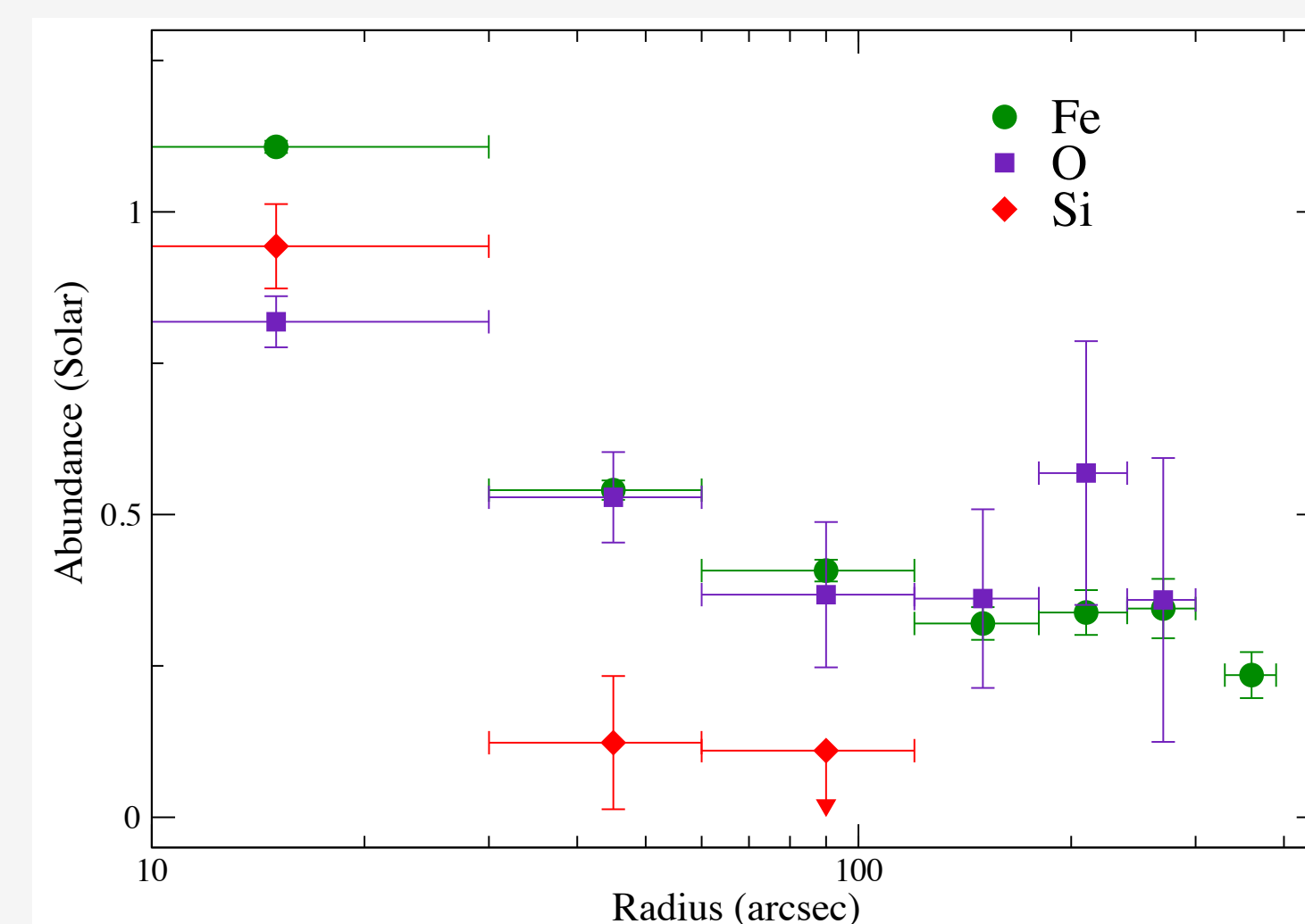
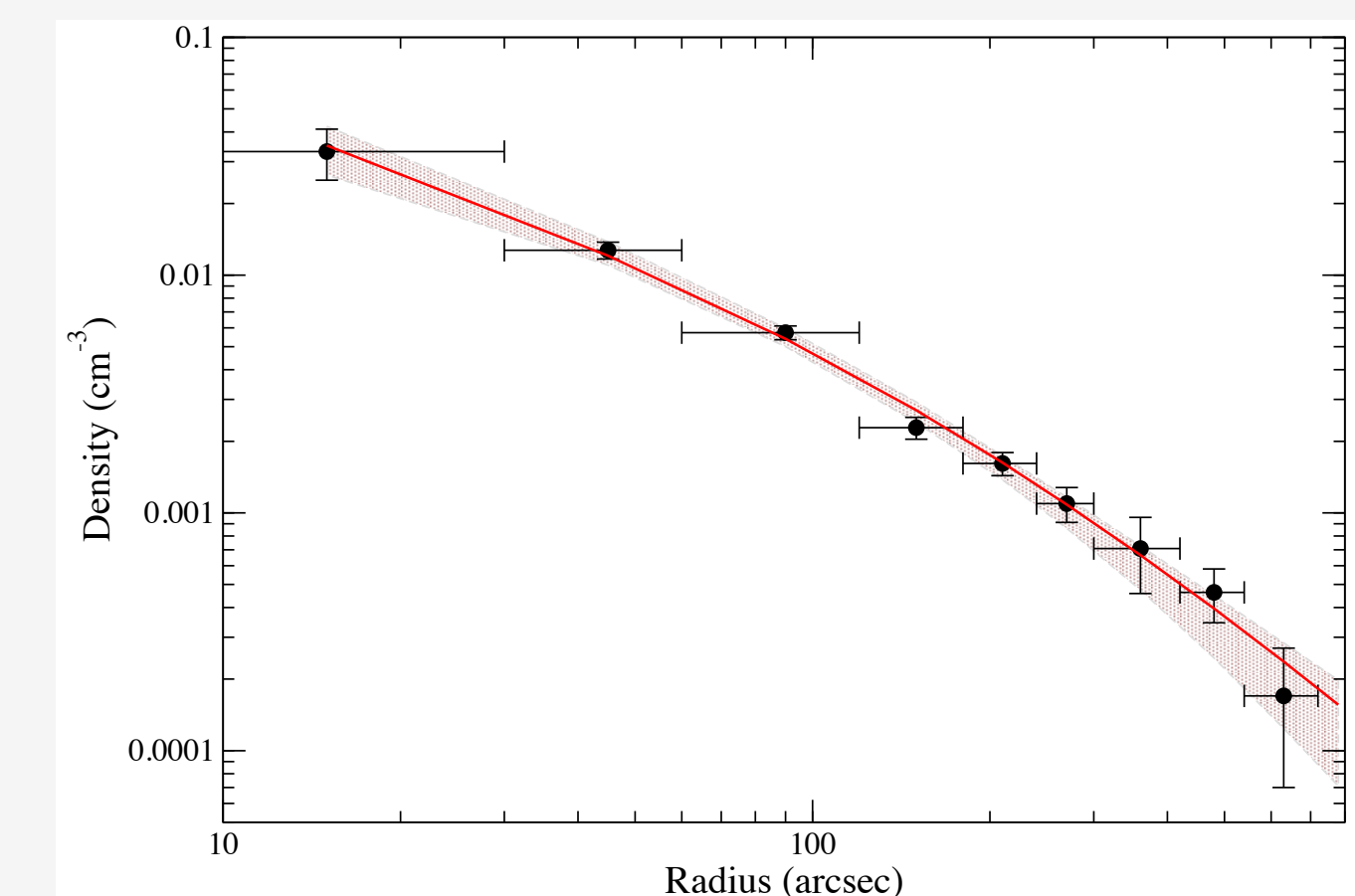


Figure 3. Centrally peaked radial distributions of Iron (Fe), Silicon (Si) and Oxygen (O) abundances with 90% confidence limits obtained from the XMM-Newton MOS and PN observations

- ◉ This best fit model obtained from Bulbul et al. (2010) model was used to determine the cluster masses (see Figure 4). The model produces the total mass of $M_{\text{tot}}=(3.00\pm 0.59)\times 10^{14} M_{\text{sun}}$ and gas mass fraction of $f_{\text{gas}}=0.149\pm 0.036$ at r_{500} .

Figure 4. The deprojected density and temperature profiles obtained from the MOS data was fit with Bulbul et al. (2010) model. The red line and the shaded area shows the best fit model ($\chi^2=13$ for 12 d.o.f.) and the 90 % confidence limit obtained from the model fit.



2- RGS Results

2.1 An Upper Limit to Thermal Broadening

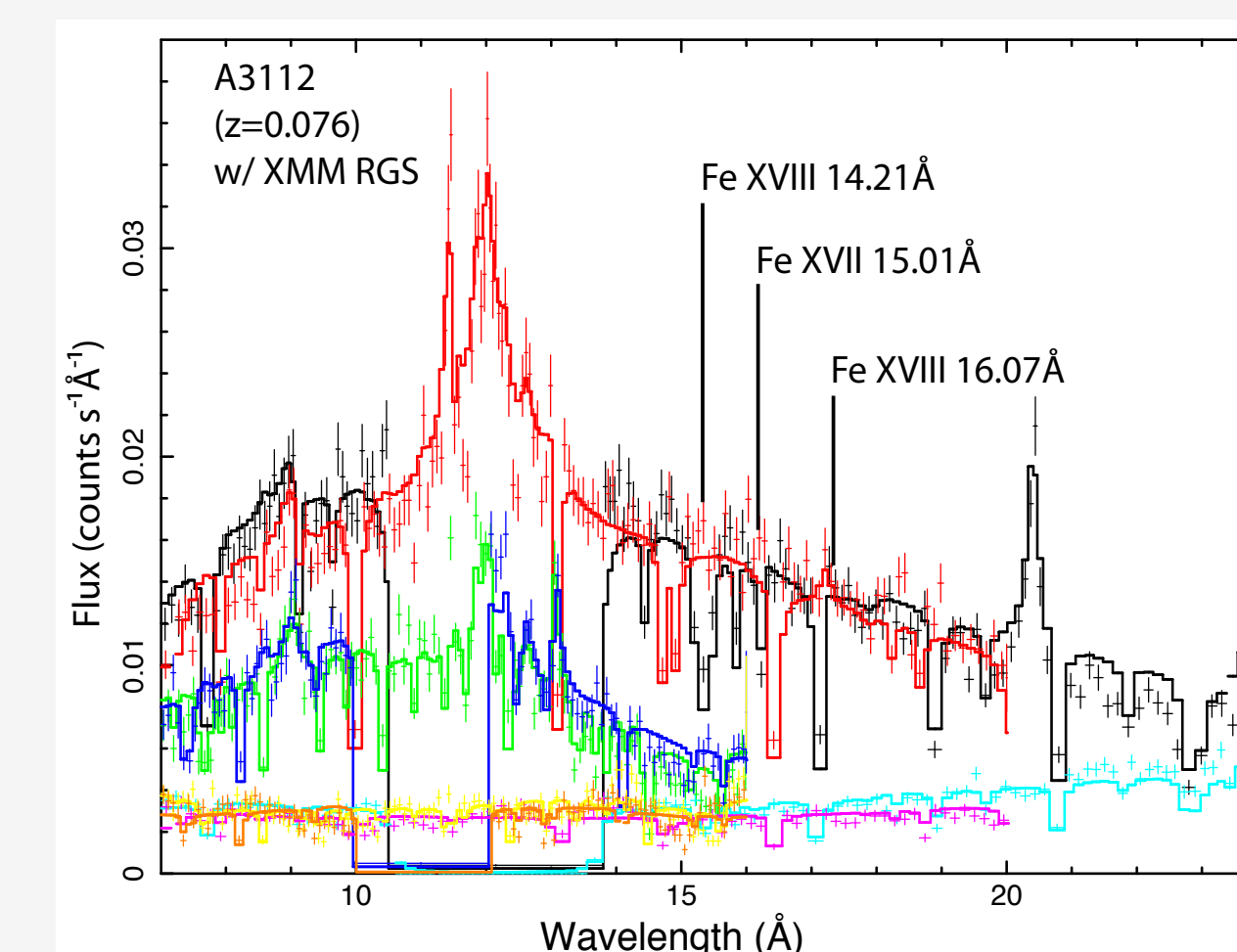


Figure 5. RGS 1st order and 2nd order spectra and background fit with a bvapec model.

- ◉ We found that the 90% upper limit to velocity broadening is 459.3 km s^{-1} by examining OVIII line region (18.5 Å-22 Å). The bvapec model fit to the RGS spectra produces the 90% upper limits to the velocity broadening of 220 km s^{-1} with the ratio of turbulent to thermal energy density less than 13.7 per cent.

2.2 Soft Excess Emission

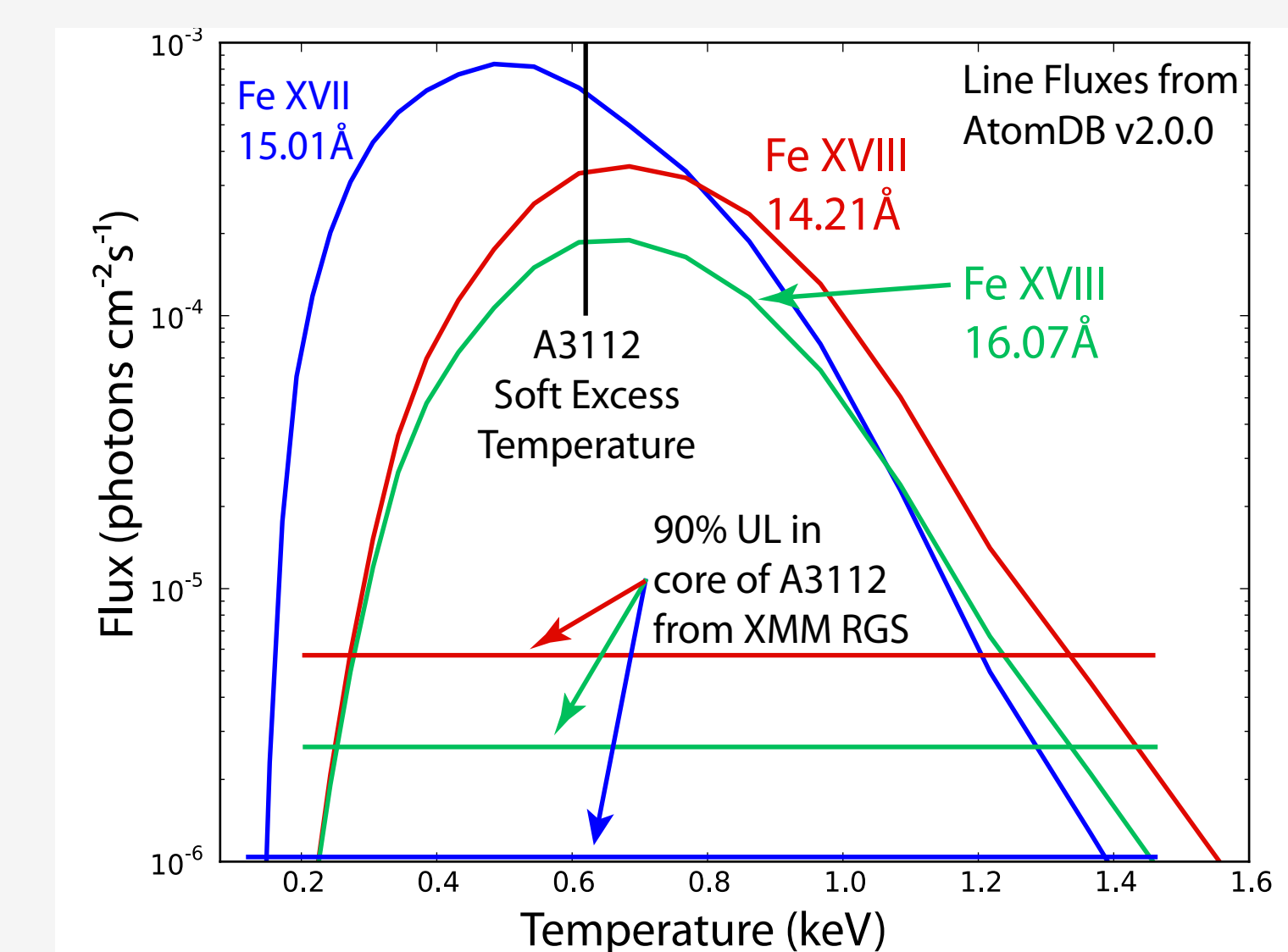


Figure 6. 90 % Upper Limits to the Fe XVII and Fe XVIII Line Fluxes obtained from the RGS observations A3112 is shown in green, red and blue straight lines. The curves shows the expected line fluxes from 0.62 keV plasma obtained from AtomDB v2.0.1.

- ◉ We also searched for the signatures of $< 1 \text{ keV}$ gas in the RGS spectra in order to test the hypothesis of the thermal origin of the soft excess detected from this cluster. The 90 per cent upper limits of Fe XVII and Fe XVIII were then compared with the line fluxes estimated using AtomDB v2.0.1 (Foster et al. 2011). The emissivity of the Fe XVII and Fe XVIII ions with predicted fluxes up to 60 orders of magnitude higher than the observed 90% upper limits obtained from RGS.

